SOLUTION MINING RESEARCH INSTITUTE
105 Apple Valley Circle
Clarks Summit, PA 18411, USA

Telephone: +1 570-585-8092
Fax: +1 570-585-8091
www.solutionmining.org

Technical Conference Paper

Subsidence, Sinkholes and Craters above Salt Caverns

Mehdi Karimi-Jafari, SOFREGAZ, Paris

Pierre Bérest, Ecole Polytechnique, Palaiseau

Benoît Brouard, Brouard consulting, Paris

SMRI Spring 2008 Technical Conference
28-29 April 2008
Porto, Portugal

SUBSIDENCE, SINKHOLES AND CRATERS ABOVE SALT CAVERNS

Karimi-Jafari M.[1], Bérest P.[2], Brouard B.[3]

[1] SOFREGAZ - 92 bd Victor Hugo, 92115 Clichy, France
[2] LMS, Ecole Polytechnique - Route de Saclay, 91128 Palaiseau, France
[3] Brouard Consulting - 101 rue du Temple, 75003 Paris, France

1. INTRODUCTION

Many papers were dedicated to sinkholes and craters above solution-mined caverns. In this paper a semi-analytical model of a cylindrical salt cavern whose roof is a stiff and competent layer is described.

1.1 Definitions

The following definitions are suggested. A *subsidence bowl* is a trough with a smooth vertical profile; the maximum gradient (or slope) of the vertical profile is several mm/m. Such a trough can be observed above any underground opening, however deep or large a cavern or mine. A *sinkhole* is a subsidence bowl whose maximum gradient is significantly larger than several mm/m. A *crater* is generated by a downward displacement of a vertical cylinder of rock; a differential vertical displacement, by several meters or dozens of meters ("step") can be observed on the edge of a crater.

A subsidence bowl, sinkhole or crater can be generated by underground "dry" mining, by natural or artificial dissolution of soluble layers, or by water or fluid pumping. In all cases, some material (fluid or rock) is removed, resulting in rock displacement and ground-surface subsidence.

1.2 Sinkholes and Craters — Examples

Sinkholes and craters are generated when several conditions are met. These conditions are related to the depth and size of the cavern, the mechanical properties of the overburden and the cavern shape. Several examples are described below.

Hundreds of salt caverns have been leached out in Lorraine (east of France). Their volume generally is from one to several 100,000 m^3. Several of them have collapsed, leading to large subsidence at ground level or even to the formation of craters, several dozens of meters deep. The collapse mechanism is well known (Buffet, 1998; Jeanneau; 2005; Boidin, 2007). When a cavern roof reaches the top of the 200-m deep salt formation, the overlying marls or anhydrite layers weather, break and fall to the bottom of the cavern. After several years, stopping ends when the cavern roof reaches a thick and stiff dolomite layer, the Beaumont Dolomite, which has a typical depth of 140 m (Buffet, 1998). When the cavern becomes large enough, this layer breaks, and a crater forms. The typical minimum diameter (at the salt/marls interface) for which cratering can occur is 120-130 m. No collapse takes place when cavern diameter is smaller than 100 m.

In the Hutchinson formation, in Kansas, the salt top of the salt formation is at a depth varying from 120 m to 300 m. Numerous mines and brine dissolution caverns, together with more than 600 storage caverns, were opened in this formation. The diameter of the storage caverns varies from 15 m to 100 m, their height from 15 m to 60 m, and their volume ranges from 1,000 m^3 to 55,000 m^3 (Poyer and Cochran, 2003). No storage cavern collapse is known, although several brine-production caverns, whose horizontal dimensions are much larger, generated dramatic collapses (Walters, 1978).

The Berkaoui salt cavern (Morisseau, 2000) inadvertently was created as a poorly abandoned oil-exploration well allowed soft water to circulate through a thick salt formation between a lower-lying prolific aquifer with a high water-head and an upper-lying aquifer. Eight years after well

abandonment, a 70-m deep, 200-m diameter crater formed at ground level. It is believed that the 450-m to 600-m deep cavern had a diameter of 300 m.

From these examples, two empirical rules can be inferred.

1. Cratering does not occur when the ratio between cavern diameter and cavern depth is significantly smaller than: $d/h \approx 2/3$.
2. Crater diameter is smaller than cavern diameter.

These "rules" need to be confirmed by further data.

1.3 Subsidence Not Related Directly to Salt Convergence

In some cases, ground subsidence is observed near salt caverns or mines, but it may not be related directly to cavern convergence. Ratigan (2000) describes the subsidence-monitoring system at Mont-Belvieu, Texas. Most of the ground subsidence is related to storage and brine-mining caverns. However, two regions over the salt dome exhibit subsidence that does not relate directly to underground caverns, but, rather, to differential movements between two spines of the salt dome.

Kunstman and Urbanczyk (2003) describe the catastrophic flooding of the Wapno Salt Mine in Poland. The brine inflow in the upper level of the mine remained small, but it continuously increased from 1970 to 1977, when it was decided to abandon the mine. Sinkholes did not develop above the mine, but 100-200 m away from the salt dome border, proving that they were related to old gypsum excavation that collapsed when water was drained toward the neighbouring mine.

Rolfs and Crotogino (2000) conducted a rock-mechanics investigation on shallow salt mines in Cheshire, UK. The aim of the study was to assess the actual stress state and bearing capacity of the rock zone surrounding the mines and to predict the subsequent surface subsidence over the long term. Measurements revealed that surface subsidence due to dissolution (at the interface of the bed salt and the upper wet marls) at the edge of the mines was higher than subsidence directly above the mines. Computations proved that the stress distribution above the mines is typical of a continuous beam: "Within the centre of the underground working, tensile stresses occur at the base of the beam and on top of the beam in the vicinity of the beam supports (in the rock area between the mines)" (Rolfs and Crotogino, 2000, p.312). Suberosion preferentially takes place in those areas where tensile stresses increased — i.e., at the mine's edge.

Feuga (2005) describes the Miéry (Jura, France) case. Here, brine production was operated with no protective salt layer at salt top (in this solution-mining method, deliberate collapse of the caverns is provoked.), and a dissolution front moved up-dip at the salt-overburden interface, leading to subsidence some distance from the brine-production field.

1.4 Negative Subsidence

"Negative" subsidence also is observed in some brine-field or hydrocarbon-storage environments. They are related to cyclic changes of aquifer waterheads or differential movements inside salt domes. They prove that interpreting subsidence data is often a tricky task.

Briggs and Sanford (2000) report "negative subsidence", or upward ground movement, observed in 1994 above the Tully Valley Brine Field, New York. This negative subsidence may be related to sealing of many wellbores, which resulted in a rise in the water table and an uplift in the rock mass.

Brennen (2001) describes cyclical motions of small amplitude (< 0.3 ft) near cavities and mines located beneath the floor of a glaciated valley filled with thick deposits of glacial drift, including aquifers. These motions correlate with natural changes in aquifer water levels.

Loof and Begnaud (2001) report upward salt movements of the salt dome as the cause of deformation of an oil storage casing at Sour Lake, Texas.

Subsidence and Cratering Analysis

Paar (2000) reviewed papers dedicated to sinkholes and subsidence published between 1960 and 2000, and stated that "*The cause and mechanism of trough subsidence and sinkhole formation is well understood and documented in many scientific papers…However, as a general rule, main emphasis is on narrative description of the occurrence itself. Quantitative descriptions or predictive tools are found to be rare or not existing*".

The theoretical or empirical basis for subsidence analysis above salt mines and salt caverns has been discussed by many authors, including Jeremic (1994), Reitze (2000), Van Sambeek (2000) and Eickemeier (2005). A good introduction can be found in Staudtmeister (2005).

Bekendam et al. (2000) propose analytical models of roof stability. They are based on the assumption that a pressure arch forms above caverns and that thin layers detach from the rock mass. Such a configuration is analysed by Obert and Duvall's (1967) modified roof-beam theory.

2.0 SEMI-ANALYTICAL MODEL

2.1 Introduction

When considering the mechanical behaviour of a salt cavern, two main cases can be considered: shallow caverns, and deep caverns. Brine-production caverns often are shallow: their diameter is of the same order of magnitude as their depth; $d/h \approx 0.5$ is typical. In deep caverns, the ratio is much lower than 0.5. The main concern here focuses on shallow caverns leached from bedded salt formations. In the following, a simplified model of an idealized cylindrical cavern whose roof can be considered as a competent elastic plate is considered (see Figure 1).

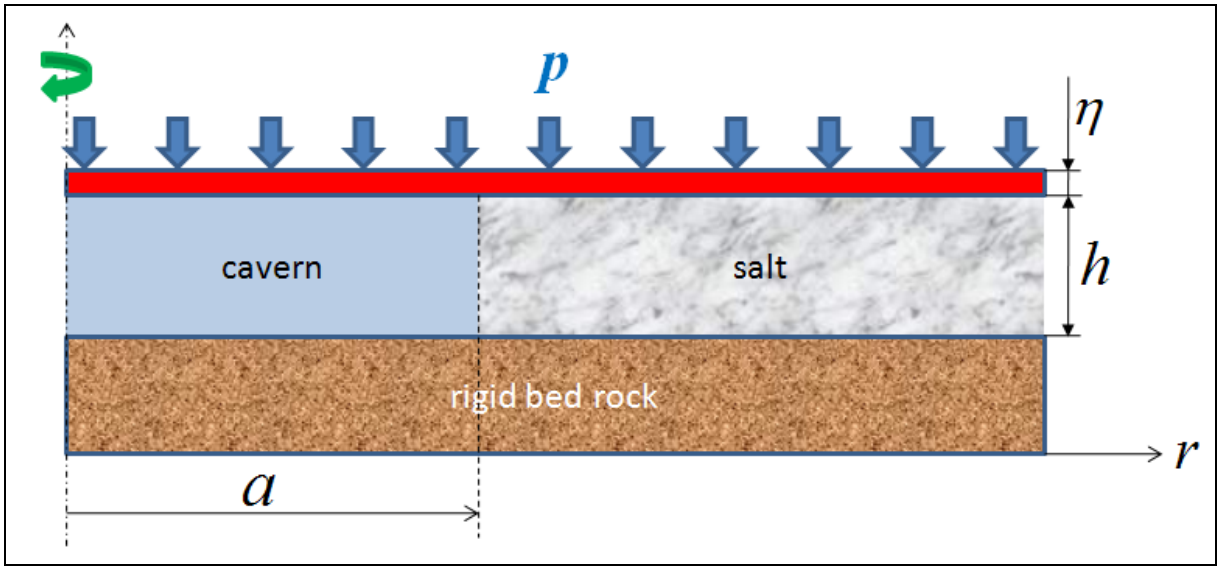

Figure 1 - Axisymmetric model of a single cavern.

The area from the bed rock to the top of the salt formation is composed of 4 layers:

(1) a rigid bed rock;

(2) a salt layer of thickness h and elastic modulus E';

(3) an elastic plate whose bending stiffness is EI, where E is the elastic modulus of the plate, $I = \eta^3 / 12$ is the bending stiffness, and η is the plate thickness; and

(4) an extremely soft layer (much softer than the elastic plate). In other words, the overburden weight is a uniform vertical load (geostatic pressure) applied on the upper surface of the plate.

Before the cavern is created, a uniform vertical load, $\sigma_0 = \gamma_R H$, is applied on the elastic plate, which is horizontal: H is the cavern depth; and γ_R is the volumetric weight of the rock mass. Brine production takes place, and a cylindrical cavern, radius $a = d/2$, is created. At the cavern roof ($r < a$), brine production results in an additional tensile vertical stress, $p = -(\gamma_R - \gamma_b)H$, applied below the elastic plate, equivalent to an additional compressive vertical stress, $p = (\gamma_R - \gamma_b)H$, applied above the plate. An additional vertical displacement, $u = u(r) > 0$, is generated, and the following relation holds in the elastic plate above the cavern:

$$EI\,\Delta\Delta u - p = 0 \qquad 0 < r < a \tag{1}$$

Above the abutment ($r > a$), no additional load is applied. However, when the elastic plate sags by u, an additional vertical stress, σ, is generated in the salt layer (thickness = h), and the salt layer thickness shortens by $u = h\,\sigma / E'$. Above the abutment, the following relation holds:

$$EI\,\Delta\Delta u + E'u/h = 0 \qquad a < r \tag{2}$$

Obviously, (2) is a simplified description of the actual mechanical behaviour of the salt layer.

Equations (1) and (2) can be solved:

In the cavern, $\quad 0 < r < a, \quad u = \dfrac{p}{64EI}\left(r^4 + Ar^2 + B\right)$

In the abutment, $\quad a < r, \quad u = C\,\mathrm{ker}\left(r/l\right) + D\,\mathrm{ker}\left(r/l\right)$

where $l^4 = EIh / E'$, A, B, C, D are four constants to be determined using boundary conditions, and *ker* and *kei* are Kelvin functions (i.e., real and imaginary parts of the solutions of the equation $\Delta u + iu = 0$). At the cavern edge, or $r = a$, the displacement u and its three first derivatives with respect to r must be continuous. These boundary conditions provide 4 equations for A, B, C and D and $u = u(r)$ — i.e., the deflection of the elastic plate can be computed easily. An example is given on Figure 2. Note that a small uplift can be observed outside the cavern edge, or $r = a$.

Stresses in the elastic plate above the cavern must be assessed. The average vertical shear stress in the plate is $\tau = pr / 2\eta$; it is largest at plate edge:

$$\tau = pa/2\eta \tag{3}$$

The additional horizontal stresses due plate bending are:

$$\sigma_t\left(r\right) = \pm 6M\left(r\right)/\eta^2 = \pm 6EI\,\Delta u/\eta^2 \tag{4}$$

The bending moment generates an additional tensile stress, $\sigma_t\left(0\right)$, below the plate at the cavern axis of symmetry; and an additional tensile stress, $\sigma_t\left(a\right)$, above the plate at the edge of the plate.

In the special case when the salt layer can be considered as extremely stiff, or $u\left(0\right) = u'\left(0\right) = 0$, the additional horizontal stress due to plate bending simply writes:

$$\sigma_t\left(r\right) = \pm 3p\left(2r^2 - a^2\right)/4\eta^2 \tag{5}$$

and additional tensile stresses are maximum in $r = 0$ and $r = a$, $\sigma_t = 3pa^2/4\eta^2$. These stresses increase when cavern radius increase, and tensile failure is more likely when cavern radius is larger. Tensile failure of the elastic plate leads to cratering, as the overburden is assumed to be much softer than the elastic plate. In fact the additional horizontal stresses must be compared to the initial

compressive stress which reigns in the plate and is equal to $\sigma_0 = \gamma_R H$. When the total stress (initial compressive stress minus additional tensile stress) is a tensile stress, tensile failure may happen – presumably at plate centre first, immediately followed by tensile failure of the elastic plate along the external profile of the cavern. When the salt layer cannot be considered as extremely stiff, Equation (4) must be used.

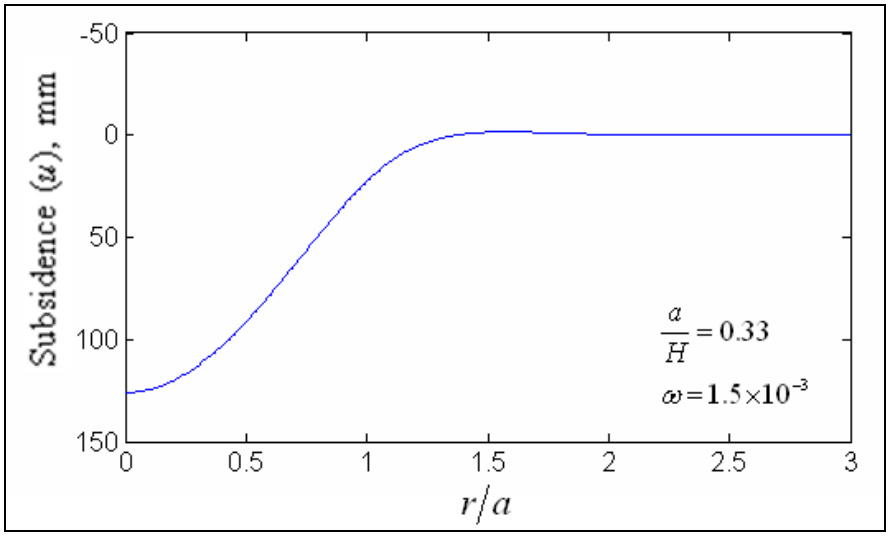

Figure 2 - Surface subsidence above the cavern.

2.2 Example

Here, we consider the case of a brine production cavern described by Buffet (1998). This cavern collapsed, and a crater was formed. The cavern top depth was $H = 150$ m, and the cavern roof was a dolomite layer $\eta = 10$-m thick. The additional tensile stress applied at cavern roof was $p = 1.8$ MPa. The Dolomite layer is considered as an elastic plate with elastic modulus $E = 45{,}000$ MPa. The cavern is a cylinder with radius $a = 50$ m. The salt layer thickness and elastic modulus equal $h = 50$ m, and $E' = 20{,}000$ MPa, respectively. Figure 2 shows the plate deflection over the salt cavern. Tensile and shear stresses in the Dolomite layer are shown in Figure 3. Shear failure mechanism is unlikely. The additional horizontal stress due to plate bending is much larger than the average vertical shear stress in the plate. (They are of the same order of magnitude for an exceedingly small cavern, $a_c \approx 3\eta^2/8H$ or 0.25 m in this case.) The maximum additional tensile stress is reached below the plate at the cavern centre. Smaller tensile stresses develop above the plate at the cavern edge.

3. PARAMETRIC DISCUSSION

In the following, we discuss the intensity of the additional tensile stress at the plate edge and at the plate centre when different values of the cavern radius are considered (Figures 4 and 5). A stiffness parameter, ω, such that $\omega = EI/E'h^3 = l^4/h^4$, was defined. For a given value of ω, the maximum additional tensile stress, σ_t/p, must be compared to the initial compressive stress, $p\gamma_R/(\gamma_R - \gamma_b)$. For a given value of the stiffness parameter, tensile failure is more likely when the cavern radius is larger.

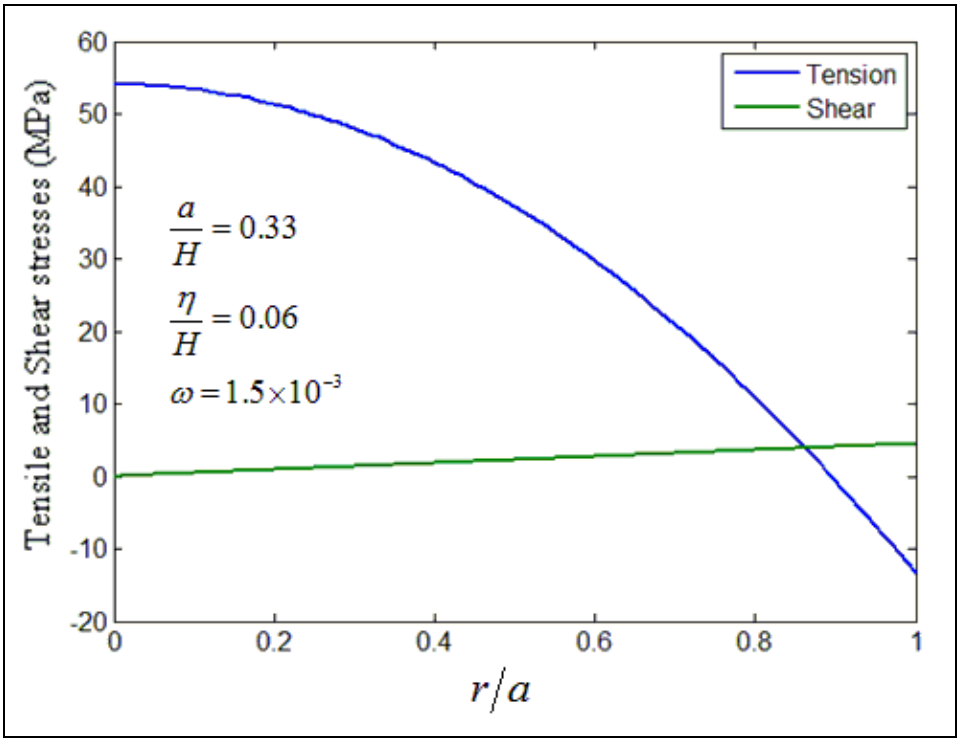

Figure 3 - Vertical shear stresses and tensile stresses on the lower surface of the plate.

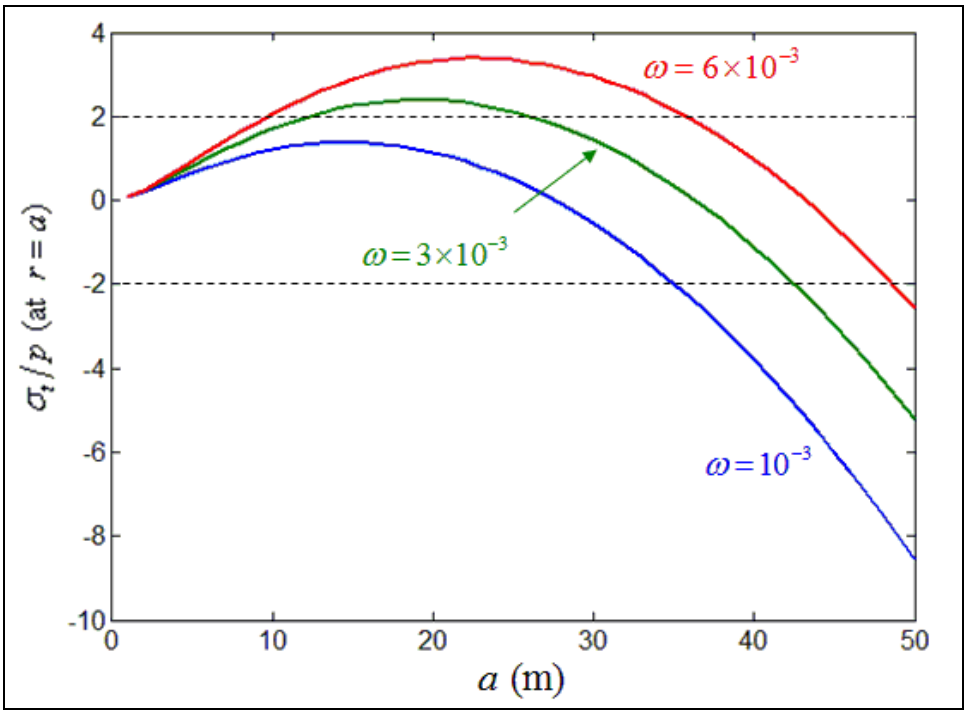

Figure 4 - Horizontal additional tensile stress at cavern edge ($r = a$).

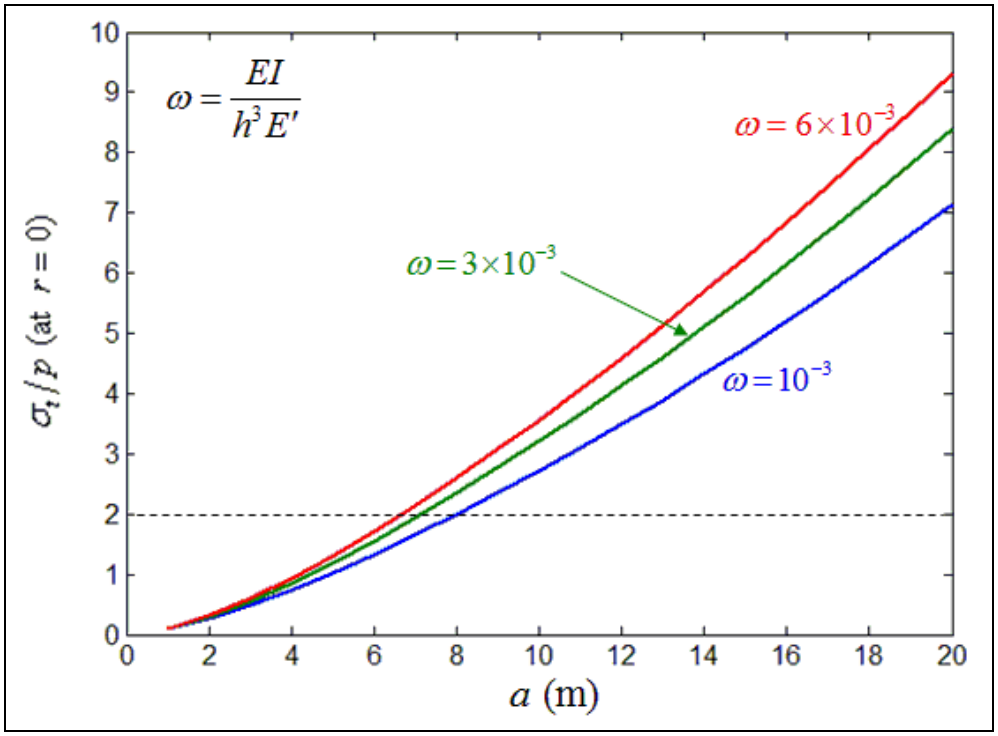

Figure 5 - Horizontal additional tensile stress at plate centre (r = 0).

4. CONCLUSIONS

A roof failure mechanism above shallow caverns has been described. The overburden strata are soft except for the cavern roof itself, which is modelled as a competent elastic plate. It is proved that tensile stresses develop in the plate and are responsible for failure initiation. Tensile stresses rapidly increase when cavern radius increases.

REFERENCES

Bekendam R., Oldenziel C. and Paar W. (2000) Subsidence Potential of the Hengelo Brine Field (Part I). Physico-Chemical Deterioration and Mechanical Failure of Salt Cavern Roof Layers. *Proc. Technical Class and Technical Session, SMRI Fall Meeting, San Antonio, p.*103-118.

Boidin E. (2007) Interactions between rocks and brines in the context of mines and caverns abandonment. *Ph.D Thesis, Institut National Polytechnique de Lorraine, February 2007* [in French].

Brennen W.J. (2001) Vertical Ground Motions Observed in Association with Salt Production in Drift-Filled Glaciated Valleys. *Proc. SMRI Spring Meeting, Orlando,* pp. 121-146.

Briggs P. and Sanford K. (2000) The Ups and downs of Post-Closure Subsidence Monitoring at the Tully Valley Brine field, New York, *Proc. Technical Class and Technical Session, SMRI Fall Meeting, San Antonio,* pp. 57-74.

Buffet A. (1998) - The Collapse of Compagnie des Salins SG4 and SG5 Drillings. *Proc. SMRI Fall Meeting, Roma,* pp. 79-105.

Eickemeier (2005) A new model to predict Subsidence above Brine Fields. *Proc. Tech. Class, SMRI Fall Meeting, Nancy.*

Feuga B. (2005) Subsidence at Miéry (Jura, France) - A case of Subsidence due to the Advance of the Dissolution of the Salt in the Up-Dip Direction. *Proc. Tech. Class, SMRI Fall Meeting, Nancy.*

Jeanneau V. (2005) The sinkhole of the cavity LR 50/51 in La Rape Area, a case history. RHODIA Company *Proc. SMRI Fall Meeting, Nancy,* pp. 9-24.

Jeremics M.L. (1994) Rock Mechanics in Salt Mining. A.A. Balkema/Rotterdam/Brookfield. p.487-530.

Kuntsman A.S and Urbanczyk K.M. (2003) Catastrophic flooding of Wapno salt Mine (1977) and controlled flooding of Solno Mine (1986-1991) – Reasons, Circumstances, Consequences. *Proc. SMRI Fall Meeting, Chester,* pp.191-200.

Loof K. and Begnaud R. (2001) Effects of Uplift and Subsidence on storage Operations, sour Lake Salt Dome – A Case History. *Proc. SMRI Spring Meeting, Orlando,* pp. 228-250.

Morisseau J.M. (2000) Uncontrolled Leaching of a Salt Layer in an Oil Field in Algeria *Proc. Technical Class and Technical Session, SMRI Fall Meeting, San Antonio*, pp. 330-333.

Obert L. and Duvall, W.I. (1967) Rock Mechanics and the design of structures in rock, *John Wiley & sons*, 650p.

Paar W.A. (2000) - Review of publications 1960-2000 on subsidence and sinkhole formation over solution-mined caverns, *Proc. Technical Class and Technical Session, SMRI Fall Meeting, San Antonio.*

Poyer C. and Cochran M. (2003) Kansas Underground Storage Regulations. *Proc. SMRI Fall Meeting, Houston,* pp.199-204.

Ratigan J.L. (2000) Anomalous subsidence at Mont Belvieu, Texas. *Proc. Technical Class and Technical Session, SMRI Fall Meeting, San Antonio,* p.38-56.

Reitze A. (2000) Prediction of Ground Movement Above Salt Caverns Using Influence Functions. *Proc. Technical Class and Technical Session, SMRI Fall Meeting, San Antonio,* p.23-36.

Rolfs O., Crotogino F. (2000) Rock mechanical problems of shallow salt mines in Cheshire, UK, *Proc. SMRI Technical class and technical session, Fall Meeting, San Antonio*, p. 304-312.

Staudmeister K. (2005) Overview of the Subject and the Technical Class Structure. *Proc. Tech. Class, SMRI Fall Meeting, Nancy.*

Walters R.F. (1978) Land subsidence in Central Kansas Related to Salt Dissolution. *Kansas Geological Survey Bulletin, 214,* pp. 1-81.

Van Sambeek L. (2000) Subsidence Modelling and Use of Solution Mining Research Institute SALT_SUBSID Software. *Proc. Technical Class and Technical Session, SMRI Fall Meeting, San Antonio,* p. 11-19.

APPENDIX — CONVERGENCE VOLUME AND SUBSIDENCE VOLUME

In a paper presented during the SMRI Nancy Meeting in 2005, Van Sambeek states that:

(1) subsidence volume is proportional to underground closure volume; and

(2) overburden often behaves as a near-continuum with uniform rock properties.

In this appendix, it is proved that when statement 2 is assumed, statement 1 is true.

An underground cavern is excavated in an infinite half-space. Ω is the rock mass, and n_i are the components of the inward unit normal at the cavern wall. Gravity forces existed before cavern creation and must not be taken into account. At the cavern wall, as a result of cavern creation, additional tensile tractions are applied. These are proportional to depth (z) and to the difference between rock volumetric weight, γ_R, and the brine volumetric weight , γ_b : $T_i = (\gamma_R - \gamma_b) z n_i$. From the equilibrium equation $\sigma_{ij,j} = 0$, it can be inferred that $(x_i \sigma_{ij})_{,j} = \sigma_{ii}$ and

$$\int_\Omega x_i T_i d\Omega = \int_\Omega \sigma_{ii} d\Omega = -3(\gamma_R - \gamma_b) HV$$

where x_i are Cartesian coordinates, V is the cavern volume, and H is the depth of the centre of gravity of the cavern.

Now, it is assumed that the rock mass is homogeneous: strain can be split into an elastic part (ε_{ij}^e) and a viscoplastic part (ε_{ij}^p). It is assumed that the viscoplastic deformation generates no rock-volume change (no dilation, or $\dot{\varepsilon}_{ii}^p = 0$); the viscoplastic strain rate vanishes to zero when the state of stress is isotropic; and the viscoplastic strain at large distances from the cavern is exceedingly small when compared to the elastic strain.

$$\dot{\varepsilon}_{ij} = \dot{\varepsilon}_{ij}^e + \dot{\varepsilon}_{ij}^p = \frac{1+\nu}{E}\dot{\sigma}_{ij} - \frac{\nu}{E}\dot{\sigma}_{kk}\delta_{ij} + \dot{\varepsilon}_{ij}^p$$

From this relation, it can be inferred that $(1-2\nu)\sigma_{ii} = E\varepsilon_{ii} = E\xi_{i,i}$, where ξ_i are the components of the displacement and

$$-\frac{3(\gamma_R - \gamma_b)(1-2\nu)HV}{E} = \int_{\partial\Omega} \xi_i n_i da$$

The rock mass boundary, or $\partial\Omega$, includes (1) cavern walls, (2) ground level, and (3) the boundary of the half-space at infinite distance from the cavern. In addition, the integral on the right-hand side can be split into three parts, each of them associated to a part of the boundary $\partial\Omega$. It can be proven that the third part of the integral (associated to the half-space boundary) is nil, that the two first parts are the convergence volume and the subsidence volume, respectively, and that

$$\frac{v_s - v_c}{V} = \frac{3(1-2\nu)(\gamma_R - \gamma_b)H}{E}$$

where v_s is the subsidence volume, and v_c is the convergence volume. In most cases, these two volumes are almost equal. For instance, H = 200 m, $(\gamma_R - \gamma_b)H$ = 2 MPa, E = 10,000 MPa, ν = 0.25, and the difference between convergence volume and subsidence volume is 0.03% of cavern volume.